EJNMMI Research
a SpringerOpen Journal

ORIGINAL RESEARCH Open Access

Detecting functional changes with [^{18}F]FAZA in a renal cell carcinoma mouse model following sunitinib therapy

David W Chapman[1,2], Hans-Sonke Jans[1], Ivy Ma[2], John R Mercer[1], Leonard I Wiebe[1], Melinda Wuest[1*†] and Ronald B Moore[1,2†]

Abstract

Background: The multitargeting tyrosine kinase inhibitor (TKI) sunitinib is currently the first-line drug therapy for metastasizing renal cell carcinoma (RCC). TKIs have profound effects on tumor angiogenesis, leading to modifications of the tumor microenvironment. The goal of this study was to determine whether these treatment-induced changes can be detected with [^{18}F]FAZA.

Methods: The present study utilized positron emission tomography (PET) to analyze tumor oxygenation status during and after sunitinib therapy in the murine Caki-1 RCC tumor model. Dynamic and static scans were performed, as well as *ex vivo* biodistributions at 3 h post injection (p.i.). Immunohistochemical analysis of tumor tissue was carried out for the quantification of pimonidazole binding and the hypoxia-associated factors CD-31, Ki-67, and Von Willebrand factor (VWF). In addition, *in vitro* cellular uptake studies were done to analyze the direct effects of sunitinib on the Caki-1 cells.

Results: During therapy with sunitinib (40 mg/kg/day), uptake of [^{18}F]FAZA into Caki-1 mice decreased by 46 ± 5% ($n = 4$; 5 days) at 3 h post injection (p.i.) during the first study and 22 ± 5% ($n = 8$; 9 days) during the long-term study, indicating a decrease in the tumor's hypoxia level. However, when drug therapy was stopped, this effect was reversed completely, and the tumor [^{18}F]FAZA uptake increased to 126 ± 6% ($n = 6$) of the control tumor uptake, indicative of an even higher level of tumor hypoxia compared to the therapy starting point. Sunitinib had no direct effect on [^{18}F]FAZA uptake into Caki-1 cells *in vitro*.

Conclusion: [^{18}F]FAZA PET could be used to monitor drug response during sunitinib therapy in RCC and may guide combination therapies based on the tumor's hypoxia status.

Keywords: Renal cell carcinoma; Tyrosine kinase inhibitor; Sunitinib; [^{18}F]FAZA

Background

Renal cell carcinoma (RCC) is the third most diagnosed urological malignancy, with 75% of cases being the clear cell RCC histological subtype [1]. RCC arises in the proximal tubule of the nephron within the kidney; its symptoms present late, often preventing diagnosis early enough to lead to a favorable prognosis [2]. The American Cancer Society estimated 65,150 new cases and 13,680 deaths in the USA in 2013, a significant increase compared to the 2005 prediction statistics of 36,160 new cases and 12,660 deaths [3,4]. Between 2005 and 2009, the overall incidence of kidney cancer in the USA increased 3.1% per year [3], which is comparable to the observed 2% increase over the past two decades worldwide and within Europe [5]. Barring early intervention, many patients will experience metastatic disease and require systemic therapy. Metastatic RCC (mRCC) rarely shows a complete and durable response to immuno- or radiation therapy [6]. Significant improvements in patient management have been achieved, however, with the development of targeted small molecules including tyrosine kinase inhibitors (TKIs) such as sunitinib, sorafenib, pazopanib, and axitinib [7-9]. Two types of TKIs are known to date. Termed type I and

* Correspondence: mwuest@ualberta.ca
†Equal contributors
[1]Department of Oncology Cross Cancer Institute, University of Alberta, 11560 University Ave, Edmonton, Alberta Canada T6G 1Z2, Canada
Full list of author information is available at the end of the article

type II, they differ in their mode of action at the ATP binding site of the tyrosine kinase [10]. Sunitinib represents a TKI of type I, which targets mainly the vascular endothelial growth factor receptor 2 (VEGFR 2) and the platelet-derived growth factor receptors (PDGFR) α and β, the stem cell growth factor c-KIT (CD117), the *RET* proto-oncogene, and the Fms-like tyrosine kinase 3 (FLT-3). In addition, sunitinib has also been shown to inhibit 72 other kinases [11,12], justifying its classification as a multitargeting receptor kinase inhibitor [13,14]. Sunitinib is currently approved for the treatment of gastrointestinal stromal tumors (GIST), pancreatic neuroendocrine tumors, and as first-line therapy for mRCC [15,16].

Sunitinib not only acts directly on tumors cells (GIST and RCC) but also indirectly by disrupting the development of blood vessels, leading to increased microenvironmental stress on the tumor tissue [12]. A number of receptor tyrosine kinases are controlled by multikinase inhibitors such as sunitinib and sorafenib. They modulate hypoxia-inducible factor 1α (HIF-1α), indicating that antiangiogenic effects might be achieved not only by direct action on vascular endothelial cells but also by blocking compensatory hypoxia- and ligand-induced changes in HIF-1α and HIF-2α expression in the target tumor cells [17]. HIF-1α levels are controlled by the oxygen tension within a cell. Under hypoxic conditions, HIF-1α is activated and, in turn, triggers the production of proteins such as VEGF, PDGF, TGF, EGF, GLUT1 and CA IX, which are all essential for angiogenesis [18,19].

Positron emission tomography (PET), a non-invasive imaging method, is a tool well suited for *in vivo* detection and characterization of hypoxia in a tumor's microenvironment [20,21]. As a clinical tool, PET can be helpful in the diagnosis, outcome prediction, and therapy monitoring of RCC cancer patients [22]. Its broader clinical utilization in this context is, however, subject to discussion [23]. Several PET radiotracers for the imaging of tumor hypoxia have been developed, such as the 2-nitroimidazoles [^{18}F]FMISO, [^{18}F]FAZA, [^{18}F]EF5, and the copper-64-based thiosemicarbazone [^{64}Cu]ATSM [24,25]. Among them, [^{18}F]FMISO is the most extensively studied and widely used PET radiotracer for quantitative assessment of tumor hypoxia in both preclinical and clinical settings [21]. [^{18}F]FAZA and [^{64}Cu]ATSM may also be useful, depending on the patient cohort. [^{18}F]FAZA, because of its lower lipophylicity and therefore faster blood and non-target tissue clearance, exhibits superior image contrast [26]. [^{18}F]FAZA and [^{18}F]FMISO yield tumor-to-kidney ratios that are similar to each other and larger when compared to [^{64}Cu]ATSM [27-29]. At present, it is unknown which hypoxia PET radiotracer would provide the greatest tumor-to-background ratio in RCC patients.

PET radiotracers were used in several clinical and numerous preclinical studies to detect tumor hypoxia and predict and analyze tumor response to chemotherapy. These tracers may play a role in guiding hypoxia-specific treatment in cancer patients [30]. Most commonly, [^{18}F]FMISO and [^{18}F]FDG were used to detect effects of a therapy with TKIs such as sunitinib or sorafenib [31-36]. To date, only one preclinical study was performed using [^{18}F]FAZA [37]. Here, the effects of gefitinib, an epidermal growth factor receptor (EGFR) inhibitor, were monitored. The current study utilizes [^{18}F]FAZA to detect functional changes in the microenvironment of a renal cell carcinoma mouse model during sunitinib therapy and subsequent withdrawal. It is known that a TKI therapy regimen, which is typically split into therapeutic fractions, induces a withdrawal flare phenomenon in RCC patients [38,39]. The goal of this study was to determine whether these treatment-induced changes in tumor hypoxia can be detected and quantified using a PET radiotracer for hypoxia in an animal model. This ability could help optimize the timing of combination therapy in metastatic RCC patients. [^{18}F]FAZA has been chosen because of its lower lipophylicity and elevated clearance.

Methods

Animal model

All animal experiments were carried out in compliance with the guidelines of the Canadian Council on Animal Care and with approval from the local Animal Care Committee of the Cross Cancer Institute under the protocol number AC 11183. Caki-1 is a human epithelial kidney clear cell carcinoma cell line which expresses the wild-type von Hippel-Lindau tumor suppressor protein and was derived from a metastatic site. Donor tumors in mice were generated by injecting approximately 100,000 Caki-1 tumor cells subcutaneously into a BALB/c nude mouse (Charles River Laboratories, Quebec, Canada). Once the tumors reached a suitable size of 400 to 500 mm^3, they were fragmented into roughly equal size of 2 × 2-mm tissue chunks and implanted into the left and right flanks of the experimental BALB/c nude mice. The tumors became palpable after 5 days, and when they reached an appropriate size of 5 to 10 mm in diameter, they were randomly assigned to the experimental groups: one receiving sunitinib therapy, the other a control group receiving vehicle injections only. Three experimental setups were performed: (A) short-term effects of sunitinib (5 days of therapy) on tumor oxygenation, (B) long-term sunitinib therapy (14 days of therapy; 5 days on, 2 days off), and (C) treatment withdrawal (another 12 days after finishing therapy). After 4, 9, and 14 days of treatment, as well as the 12 days after treatment withdrawal, selected mice from both groups were analyzed with PET. Sunitinib malate (Sutent™) was a gift from Pfizer Canada (Kirkland, Quebec, Canada). The mice in the treatment groups received intraperitoneal injection of 40 mg/kg/day of sunitinib malate

in saline/1%DMSO; the control groups received vehicle injections (saline/1%DMSO).

Positron emission tomography

PET detection of tumor hypoxia was performed on BALB/c nude mice bearing subcutaneous Caki-1 tumors following the injection of 1-(5-deoxy-5-[^{18}F]fluoro-α-D-arabinofuranosyl)-2-nitroimidazole ([^{18}F]FAZA). Radiosynthesis of [^{18}F]FAZA was performed in automated synthesis units according to a standard literature procedure [40]. The precursor for the [^{18}F]FAZA synthesis, 1-(2,3-diacetyl-5-tosyl-(α-D-arabinofuranosyl)-2-nitroimidazole, was purchased from ABX GmbH (Radeberg, Germany). For PET experiments, a catheter was placed into the tail vein of the sedated mouse. Under inhalation anesthesia, the mice were placed in prone position with their medial axis parallel to the axis of the microPET® R4 scanner (Siemens Preclinical Solutions, Knoxville, TN, USA) and their thorax, abdomen, and hind legs centered in the field of view. A transmission scan for attenuation correction was not acquired. [^{18}F]FAZA (4 to 5 MBq in 100- to 150-μL solution - H_2O/max. 8% EtOH and diluted with normal saline (NS)) was injected intravenously through the catheter into the tail vein. For the different experimental protocols, an emission scan of either 180-min (dynamic experiments in setup A) or 10-min (static scans in setup B) PET acquisitions was subsequently performed. The dynamic list mode data were sorted into sinograms with 65 time frames (10×2, 8×5, 6×10, 6×20, 8×60, 10×120, 5×300, and 12×600 s). The frames were reconstructed using ordered subset expectation maximization (OSEM) or maximum *a posteriori* (MAP) reconstruction modes. The pixel size was $0.085 \times 0.085 \times 0.12$ cm, and the resolution in the center field of view was 1.8 mm. Correction for partial volume effects was not performed. The image files were further processed using the ROVER v2.0.51 software (ABX GmbH). Masks defining 3D regions of interest (ROI) were set, and the ROIs were defined by thresholding. ROIs covered all visible tumor mass of the subcutaneous tumors, and the thresholds were defined by 50% of the maximum radioactivity uptake level of each Caki-1 tumor in each animal. Mean standardized uptake values (SUV_{mean} = (activity/mL tissue)/(injected activity/body weight), mL/g) were calculated for each ROI. For comparison, SUV_{max} was also analyzed for the static PET experiments. Time-activity curves (TAC) were generated for the dynamic scans only. All semi-quantified PET data are presented as means ± SEM.

After each PET scan, the mice were immediately sacrificed by cervical dislocation, and the tumors and muscle tissue were collected in scintillation vials, weighed, and counted using a Wizard-3 1480 automatic gamma counter (Perkin-Elmer Life Sciences, Woodbridge, ON, Canada). Biodistribution experimental results were analyzed as percentage of injected dose per gram of tissue (%ID/g) or as SUV. All biodistribution values were obtained at 3 h post injection (p.i.) of the radiotracer. Data are presented as means ± SEM.

Kinetic modeling

Based on investigations by Verwer et al. [41], a reversible two-tissue compartment model with blood volume parameter was applied to the data sets. For this purpose, an ROI defining the heart content was generated by thresholding the averaged early time frames which visualized the blood flow through the heart. The plasma input TAC generated from this ROI was convolved with the compartmental model and numerically fitted to the tumor TACs of the same animal. This procedure was implemented in Matlab software (version R2014a), utilizing a Nelder-Mead simplex direct search. The fit was governed by the minimization of the sum over all time points of square differences between the measured values and the model prediction.

Immunohistochemistry

Following euthanization, the tumor tissue samples were collected for preparation of formalin-fixed paraffin-embedded tissue slides. One hour (short-term experiment with 5-day sunitinib treatment only) or 3 h (long-term experiment with 14 days of sunitinib therapy plus therapy withdrawal) prior to sacrificing the animal, pimonidazole HCl (Hypoxyprobe, Inc., Burlington, MA, USA) was injected intraperitoneally at a dose of 60 mg/kg. Additionally, immunostaining for platelet endothelial cell adhesion molecule (PECAM) CD-31 (rabbit polyclonal anti-mouse CD-31, Santa Cruz Biotechnology Inc., Dallas, TX, USA), Von Willebrand factor (rabbit polyclonal von Willebrand factor antibody), and Ki67 (rabbit monoclonal anti-mouse Ki67, Abcam Inc., Toronto, ON, Canada) were performed to illustrate changes in neoangiogenesis and vascular density. Briefly, following rehydration and antigen retrieval, endogenous peroxidase activity was blocked using methanol containing 0.3% hydrogen peroxide. After that, the sections were incubated for 1 h with the subsequent primary monoclonal antibody. The bound antibodies were visualized using DakoCyomation Envision-horseradish peroxidase and chromagen using the EnVision™ FLEX kit (Dako Canada, Burlington, Ontario, Canada). The slides were counterstained with hemotoxylin and analyzed under a microscope (Axiocam HR, Zeiss, Oberkochen, Germany). The images were edited with Adobe® Photoshop (Adobe Systems Inc., San Jose, CA, USA) to remove connective and non-tumor tissue surrounding the tumor. Then, using MetaMorph® Microscopy Automation & Image Analysis Software (Molecular Devices, LLC, Sunnyvale, CA, USA), color thresholds were defined for the entire tumor area and the specific antibody bound tissue only. Percent of

binding was calculated from the resulting number of pixels for each of the investigated factors.

In vitro cell uptake

The human renal cell carcinoma cell line, Caki-1 (American Tissue Cell Culture (ATCC)), and for comparison, the human mammary carcinoma cell line MCF-7 (a gift from Dr. David Murray, Cross Cancer Institute, University of Alberta) were used. The cell lines were cultured at 37°C and 5% CO_2 (standard conditions) in F-12/DMEM medium supplemented with 10% fetal bovine serum, 2 mM glutamine, 1% penicillin/streptomycin, 10 mM HEPES, 1 mM sodium pyruvate, and 1% non-essential amino acids. Using glass cell culture dishes with a diameter of 55 mm, the cells were plated at a density of approximately 500,000 cells per plate and incubated for 48 h under normal conditions at 37°C and 5% CO_2. Following that time, half of the plates were taken for culturing the cells under hypoxic conditions over the next 24 h; the others were kept under normal cell culture conditions. Hypoxic cell culture conditions were achieved using a special sealed vacuum chamber device (Division of Experimental Oncology, Department of Oncology, University of Alberta) in which O_2 was almost entirely replaced with N_2 ($O_2 < 0.1\%$) [42]. For the radiotracer incubation, the medium was replaced with Krebs-Ringer buffer (115 mM NaCl, 5.9 mM KCl, 1.2 mM $MgCl_2$, 1.2 mM NaH_2PO_4, 1.2 mM Na_2SO_4, 2.5 mM $CaCl_2$, 25 mM $NaHCO_3$, and 5 mM glucose at a pH of 7.4) at room temperature. Around 2.5 to 3.5 MBq of [^{18}F]FAZA, containing buffer was added per plate and incubated for 4 h under either normal or hypoxic conditions. Sunitinib maleate 90 μL of 10^{-4} M (in DMSO) was added to selected plates to analyze the effect of sunitinib on cellular [^{18}F]FAZA binding. After incubation, the cells were rinsed three times with ice-cold Krebs-Ringer buffer to stop further cell uptake and then immediately lysed using 1 mL 5% trichloroacetic acid (TCA) for 1 h. One plate of each condition was used for protein quantification using the BCA protein assay kit (Pierce, Rockford, IL, USA) according to the manufacturer's recommendations, and bovine serum albumin was used as the protein standard. Following the 1-h lysis with TCA, the supernatants were collected and placed into scintillation vials to be counted using the Wizard gamma counter (Wallac 1480 Wizard-3, Perkin-Elmer) in order to determine radioactivity uptake levels in the cells. Radiotracer cell uptake levels were normalized to percent of the total added radioactivity per milligram protein (% radioactivity/mg protein). Data are presented as means ± SEM.

Results

Effect of sunitinib on Caki-1 tumor growth

Figure 1 summarizes the Caki-1 tumor growth over a 40-day period based on all mice used for the long-term therapy protocol with additional therapy withdrawal. The tumors were allowed to grow for 13 days until therapy with sunitinib was started. After therapy was started on day 13, tumor growth in the treatment group decreased over the next 2 weeks. After therapy, withdrawal tumor growth rates still differed; however, at the end of the study at day 40, the tumor sizes between both groups were comparable again, indicating an increased tumor growth rate in the treated group (tumor growth flare).

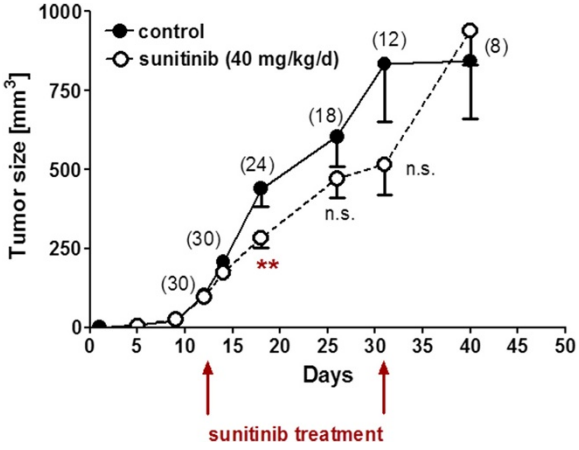

Figure 1 Caki-1 tumor growth curves over 40 days. Data from all mice are included; mouse numbers are shown in brackets. Sunitinib (40 mg/kg/day) treatment started on day 13 and finished on day 31. Data are shown as mean ± SEM. $^{**}p < 0.01$; n.s., not significant.

Characterization of the Caki-1 tumor model with [^{18}F]FAZA

Prior to determining the effects of a sunitinib therapy on Caki-1 tumor's oxygenation, the hypoxia tracer [^{18}F]FAZA was used to evaluate the basic hypoxia characteristics of this preclinical RCC model. Figure 2 shows selected PET images at 30 min and 2 and 3 h p.i. from 3-h dynamic acquisitions. The generated TACs for the uptake profile of [^{18}F]FAZA in tumor and muscle tissue, as well as the subsequent tumor/muscle ratios over 3 h, are shown at the bottom of Figure 2. The TACs revealed a rapid uptake of [^{18}F]FAZA into the tumor tissue and resulted in an SUV_{mean} of 0.35 ± 0.03 after 1 h p.i. and an almost unchanged SUV_{mean} of 0.32 ± 0.02; $n = 6$ tumors/three mice after 3 h p.i. The overall [^{18}F]FAZA uptake into the Caki-1 tumor cells seemed to be very low, indicating lower levels of hypoxia. However, [^{18}F]FAZA also cleared from the muscle tissue over time ($SUV_{mean,3h,}$ 0.23 ± 0.04; $n = 6/3$), leading to an increased tumor/muscle ratio over time from 1.10 ± 0.03 at 1 p.i. to 1.56 ± 0.12 ($n = 6$) after 3 h p.i. This analysis confirmed that after 3 h p.i., the subcutaneous Caki-1 model may possess an optimal tumor/background ratio sufficient for static PET image analysis.

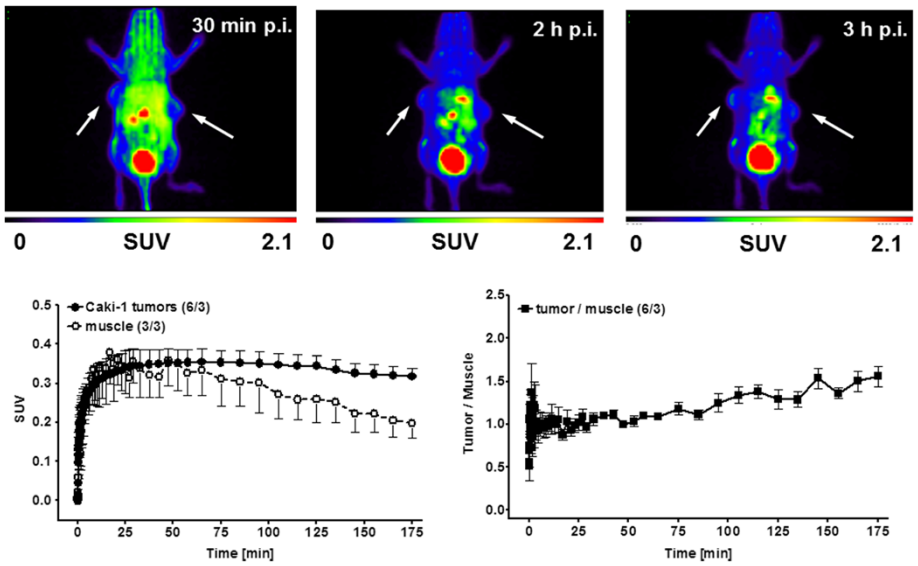

Figure 2 Dynamic [^{18}F]FAZA images in a BALB/c nude mouse bearing two Caki-1 tumors. Time-activity curves for the radioactivity uptake into Caki-1 tumor and muscle tissue as well as the tumor/muscle ratios (bottom). Image data are presented as maximum intensity projections (MIP) at 30 min, 2 and 3 h post injection. Data in TACs as SUV and mean ± SEM from six tumors out of three mice and three regions of muscle from those three mice.

Effect of sunitinib on [^{18}F]FAZA uptake and trapping *in vivo*

Following the characterization of the Caki-1 RCC model, [^{18}F]FAZA PET was used to detect the effects of sunitinib on the tumor's hypoxia. Five days of sunitinib (intraperitonial injection) led to a decrease in [^{18}F]FAZA tumor uptake (Figure 3). As dynamic PET experiments revealed, lower levels of radiotracer were detected and these decreased over the 3-h time frame. In treated animals, [^{18}F]FAZA uptake into the Caki-1 tumors reached its maximum at 30 min p.i. (SUV_{mean} of 0.38 ± 0.02 (n = 4/2)) and decreased to a final $SUV_{mean,3h}$ of 0.23 ± 0.02 (n = 4/2; $p < 0.05$). In control tumors, a SUV_{mean} of 0.44 ± 0.05 was measured after 60 min and 0.42 ± 0.05 (n = 4 tumors/two mice) after 3 h p.i. This observation showed clearance of [^{18}F]FAZA and therefore less trapping of the radiotracer, indicative for a lower level of hypoxia in the treated versus the non-treated tumors. Biodistribution analysis of tumor tissue after the PET experiments confirmed these findings: 2.20 ± 0.30% ID/g in the controls versus 1.38 ± 0.13% ID/g (n = 8/4; $p < 0.05$) in the sunitinib-treated tumors.

Uptake and retention of [^{18}F]FAZA in Caki-1 tumors was further analyzed by kinetic modeling using a two-compartment model [41]. All four kinetic parameters k_1 to k_4 were calculated for control as well as for the sunitinib-treated tumors (Figure 3, bottom right). In the presence of sunitinib, all constants were found to be increased, significantly even for k_2 and k_4 with a $p < 0.05$. Once diffused into the cell, [^{18}F]FAZA either diffuses back out of the cell or is reduced for further intracellular binding. The first process is governed by the rate constant k_2 and is elevated under sunitinib therapy, as is the latter, which is governed by k_3. The ratio $k_3/(k_2 + k_3)$, however, remains unchanged, indicating that once it has crossed the cell membrane, a similar fraction of [^{18}F]FAZA will be further reduced in the presence or absence of sunitinib. Once reduced, re-oxygenation of [^{18}F]FAZA is governed by the rate constant k_4. It is amplified in the presence of sunitinib, resulting in the observed reduction in uptake under treatment (Figure 3). Analysis of the fractional blood volume (fbv) revealed similar values in the absence and presence of sunitinib: 0.160 ± 0.032 and 0.148 ± 0.036 (n = 4), respectively, indicating similar overall perfusion of the tumor volume (yet not necessarily the microenvironment, which can display hypoxia).

Following PET imaging and biodistribution experiments, tumor tissue slices were analyzed immunohistochemically. Figure 4 summarizes the results for pimonidazole, CD-31, VWF, and Ki67 staining. Treatment of Caki-1 tumor-bearing mice with sunitinib led to reduced staining of Ki67, CD-31, and an increase in VWF. Although no significant difference in the quantification of the pimonidazole staining was detectable, a qualitative trend of decreased staining density was observed in the long-term study (see Figure 5). A potential reason for this observation could be that animals were sacrificed at 1 h p.i. of pimonidazole for the short-term experiments. Since pimonidazole, like FAZA, is a 2-nitromidazole, no effects of sunitinib were detected after 1 h p.i. in accordance with the PET results (Figure 3). A 1.83 ± 0.10% CD-31 binding was determined

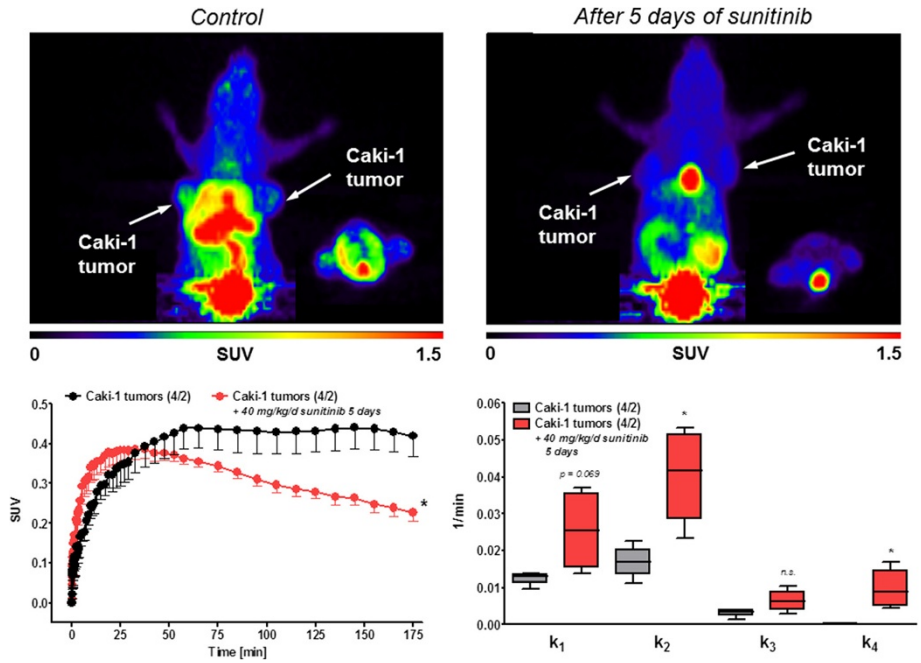

Figure 3 [^{18}F]FAZA images in Caki-1 tumor mice in the absence (left) and presence (right) of sunitinib. The insets show the respective transaxial slides of both mice. Time-activity curves for the radioactivity uptake into Caki-1 tumor in the absence and presence of sunitinib *in vivo* (bottom left). Image data are shown as maximum intensity projection (MIP) at 3 h post injection and TAC data as SUV and mean ± SEM from four tumors grown in two mice. Kinetic constants k_1 to k_4 were calculated based on a two-compartment model (bottom right). Changes were significant for k_2 and k_4 (*$p < 0.05$).

in the tumor tissue from the control mice, whereas the samples from sunitinib-treated animals showed reduced binding of 0.58 ± 0.05% CD-31 ($n = 8/4$ - tumors from four mice; $p < 0.001$). Additionally, in the controls, 0.53 ± 0.05% VWF positive cells were found versus 0.31 ± 0.08% in sunitinib-treated samples ($n = 8/4$; $p < 0.001$). Ki67 immunohistochemistry showed a decreased binding from 75 ± 2% Ki67 positive cells in the controls to 54 ± 6% Ki67 positive cells in the treated samples ($n = 8/4$; $p < 0.001$).

Monitoring therapy effects and withdrawal of sunitinib with [^{18}F]FAZA

Following the investigation of short-term effects of sunitinib on tumor oxygenation, a second experimental series was performed in order to analyze the longitudinal effects of anti-angiogenic therapy on Caki-1 tumor oxygenation. Figure 5 summarizes the PET results with [^{18}F]FAZA for the effect of sunitinib during the therapy and after therapy withdrawal. Treated Caki-1 tumors clearly showed higher radioactivity uptake levels than the control tumors, confirming that in the presence of sunitinib, the amount of tumor hypoxia is decreased in the tumor microenvironment. After 9 days of sunitinib therapy (Figure 5, left), the $SUV_{mean,3h}$ of control tumors was found to be 0.24 ± 0.02, while the $SUV_{mean,3h}$ of sunitinib-treated tumors was 0.19 ± 0.01 ($n = 8$; $p < 0.05$). Similar results were obtained when analyzing SUV_{max} values, which are more relevant for clinical use: 0.38 ± 0.03 (control) versus 0.29 ± 0.02 (9 days of sunitinib; $n = 8$, $p < 0.05$). Pimonidazole staining from tissue slices confirmed a reduction in hypoxia of the treated tumors. Twelve days after sunitinib therapy was withdrawn, [^{18}F]FAZA uptake into the treated tumors increased again, leading now to even higher uptake levels than the control tumors (Figure 5, right): $SUV_{mean,\ 3\ h}$ of 0.18 ± 0.01 (control) versus 0.23 ± 0.01 (sunitinib-treated; $n = 6$, $p < 0.05$). Analysis of SUV_{max} revealed the following values: 0.30 ± 0.02 (control) versus 0.36 ± 0.02 (after therapy withdrawal; $n = 6$, $p < 0.05$). This was indicative of higher levels of hypoxia and corresponded to a flare effect after withdrawal of sunitinib. The pimonidazole staining confirmed this phenomenon with similar levels of binding in both the control and the treated groups.

In vitro cell uptake

In order to assess the overall functional effects of a sunitinib treatment *in vivo*, uptake of [^{18}F]FAZA into the Caki-1 cells was analyzed directly in the absence and presence of sunitinib *in vitro*. Hypoxia selective uptake and retention (= trapping) of [^{18}F]FAZA occurs only under hypoxic conditions. After a 4-h incubation time, [^{18}F]FAZA uptake was significantly higher in the Caki-1 cells (Figure 6): 2.42 ± 0.09% (hypoxia) versus 0.24 ± 0.02% radioactivity/

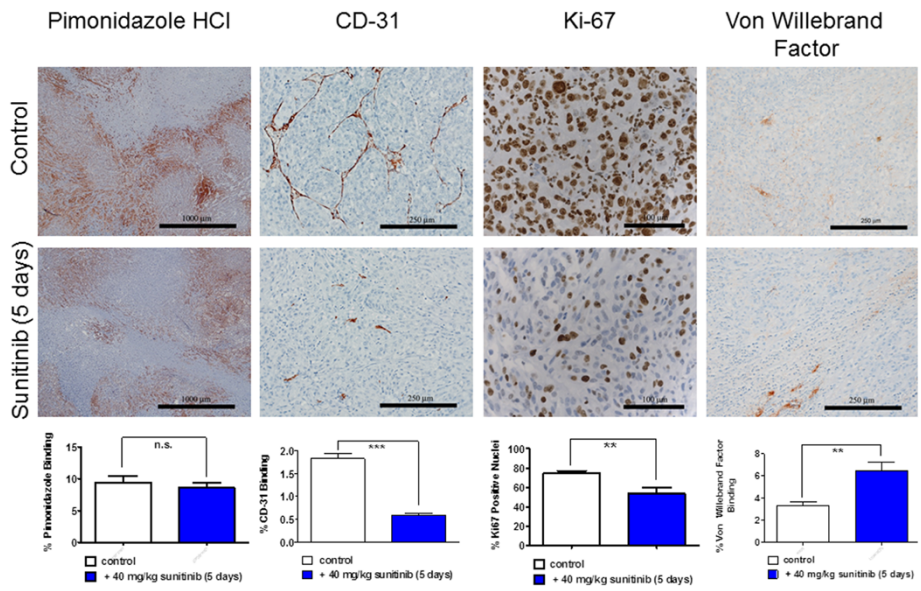

Figure 4 Immunohistochemical staining with pimonidazole HCl, CD-31, Ki-67, and VWF in Caki-1 tumor tissue slices. Slices are shown from control animals and mice treated with sunitinib (40 mg/kg/day) for 5 days (top). Quantified staining data for the percent positive stained tissue. Data as mean ± SEM with $^{**}p < 0.01$; $^{***}p < 0.001$ and n.s. for not significant.

mg protein ($n = 9$; $p < 0.001$; normoxia). For comparison and proof of the experimental setup, MCF-7 cells, known to have a higher uptake of the hypoxia PET tracer under hypoxic conditions, were also analyzed: 2.63 ± 0.44% (hypoxia) versus 0.37 ± 0.06% radioactivity/mg protein ($n = 9$; $p < 0.001$; normoxia). Cellular trapping of [^{18}F]FAZA into the Caki-1 and MCF-7 cells was increased approximately eightfold to tenfold under hypoxic conditions, confirming increased cellular retention of [^{18}F]FAZA under hypoxic conditions. The presence of sunitinib (3 μM) did not change the uptake properties of [^{18}F]FAZA into the cell lines (Figure 6), indicating no direct effect occurring from this compound on the cellular uptake of a hypoxic radiotracer.

Discussion

Four main findings of the current study may be summarized as follows: (i) xenograft Caki-1 RCC tumors show

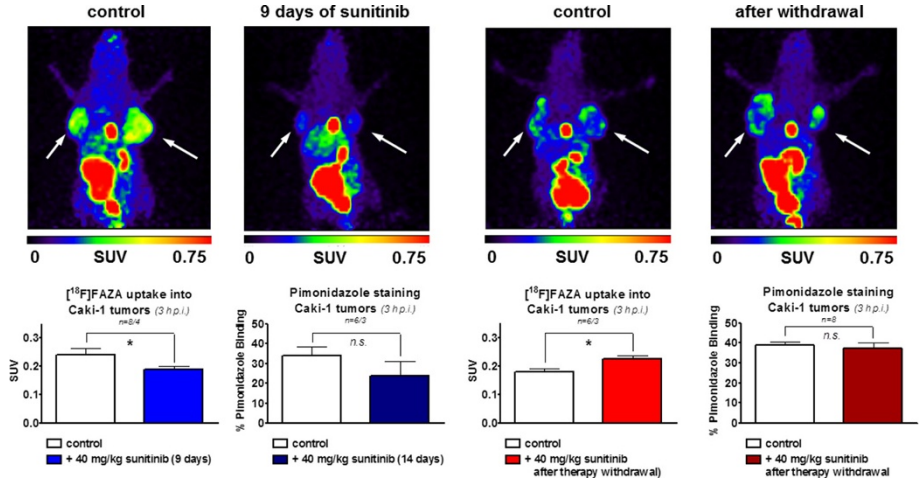

Figure 5 Static [^{18}F]FAZA images in BALB/c nude mice bearing two Caki-1 tumors on each upper flank. Image data are presented as maximum intensity projection (MIP) at 3 h post injection. Top left: control mouse versus sunitinib-treated mouse (9 days 40 mg/kg). Top right: control mouse versus a sunitinib-treated mouse which had received 13 days of drug therapy followed by 12 days after therapy was finished. Bottom: semi-quantified PET data as SUV in comparison to percent pimonidazole binding in tumor slices. Data as mean ± SEM from *n* analyzed tumors grown in *x* mice. $^{*}p < 0.05$.

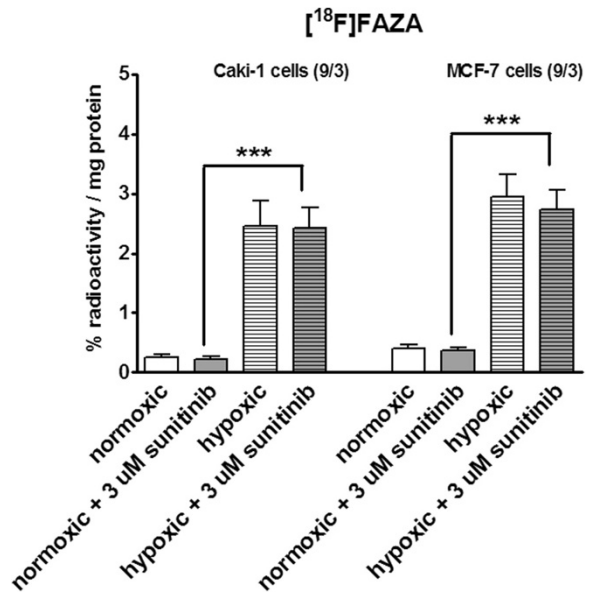

Figure 6 Uptake of [^{18}F]FAZA into Caki-1 (renal cell carcinoma) and MCF-7 cells (human breast cancer cell line). Cell uptake was normalized to percent radioactivity per milligram protein, and data are shown as mean ± SEM from *n* analyzed cell culture dishes from *x* number of experiments. Cell uptake was measured under normoxic and hypoxic conditions and in the presence and absence of 3 μM sunitinib.

uptake of [^{18}F]FAZA, revealing a base level of hypoxia; (ii) sunitinib therapy reduces [^{18}F]FAZA tumor uptake, indicating reduced tumor hypoxia; (iii) TKI withdrawal flare phenomenon was observed after sunitinib was discontinued, resulting in a once more increased tumor hypoxia; and (iv) sunitinib did not influence the direct cellular uptake and retention of [^{18}F]FAZA in the Caki-1 and MCF-7 cells under normoxic or hypoxic conditions *in vitro*.

Currently, treatment of metastatic RCC with the TKI sunitinib is recommended as one of the first therapy options [7,15,16]. Sunitinib causes reduced tumor size or growth rate. In the current study, smaller Caki-1 tumor sizes were observed in the treated mice. Meta-analysis of metastatic RCC studies has shown that higher exposure to sunitinib is correlated with improved treatment outcomes. Patients with the highest exposure to sunitinib had longer times to progression, and the probability of decreases in tumor size or of halting tumor growth was higher in patients with the highest exposure to sunitinib [16,43]. However, after therapy, Caki-1 tumors reached similar sizes again, indicating that the tumors regained their molecular characteristics which are essential for tumor development and growth. Changes occurring during therapy with sunitinib seem to be reversed after treatment disruption, leading to further tumor progression. The goal in patients would be to have a maximum exposure time to sunitinib which is associated with longer time to tumor progression, longer overall survival, and greater decrease in tumor size [43].

Therapy of metastatic RCC with TKIs can be monitored with non-invasive imaging methods to analyze therapy success as well as predict patient outcomes [22,23]. Several preclinical and clinical studies have been carried out to analyze therapeutic effects of a TKI such as sunitinib or sorafenib utilizing PET [31-38]. Besides monitoring tumor metabolism in RCC with [^{18}F]FDG, [^{18}F]FMISO was used to analyze effects on tumor oxygenation status and [^{18}F]FLT for determination of proliferation. During the present study, [^{18}F]FAZA was used. Although [^{18}F]FAZA in comparison to [^{18}F]FMISO may exhibit a better clearance pattern from non-targeting muscle tissue based on its lower lipophylicity, there is still a debate about the radiotracer of choice for imaging tumor hypoxia [26-28]. In Caki-1 tumors, [^{18}F]FAZA uptake amounted to 1.5% to 2.2% ID/g after 3 h p.i. As analyzed from the dynamic PET studies, initial uptake reached a maximum level after approximately 40 to 60 min which did not further increase. Image contrast with [^{18}F]FAZA is achieved based on the non-target tissue clearance over time. In Caki-1 tumors, a tumor-to-muscle ratio of approximately 1.5 was reached after 3 h p.i.. The current findings are in line with observations in other murine and human xenograft models of different origin, where 1.3% to 3% ID/g or even lower levels were measured at the same time p.i. [26,27,44]. Similar to the Caki-1 model, low uptake of [^{18}F]FMISO was found in A498, another human RCC xenografted tumor model [33].

PET is an ideal non-invasive imaging tool to use for monitoring response to therapy. However, there are still ongoing discussions of how patients would benefit from monitoring tumor hypoxia status and how hypoxia-directed therapy approaches could be used clinically [30,45]. During the present study, sunitinib therapy led to a reduction of tumor hypoxia levels by 22% to 46% as determined with [^{18}F]FAZA. Although sunitinib mainly targets tumor vasculature and function, it can be concluded that it also leads to a reduction of tumor hypoxia. As Verwer et al. [41] have proposed, a reversible two-tissue compartment model best describes uptake through passive diffusion and initial retention based on a chemical reduction of a nitroimidazole such as [^{18}F]FAZA. Both steps are reversible: higher oxygen levels can re-oxygenate the reduced radiotracer, and [^{18}F]FAZA may leave cells again via diffusion into the plasma. Kinetic analysis of the present dynamic data revealed that k_1 to k_4 were all elevated in the presence of sunitinib, k_2 and k_4 even significantly. Increased k_1 shows that sunitinib-treated tumors allow even faster cellular uptake of [^{18}F]FAZA. Delivery of the radiotracer through the tumor vasculature is rather improved and not impaired. On the other hand, elevated

k_2 indicates a higher rate of back diffusion into the plasma for treated mice. One can conclude that in this case, more re-oxygenated [^{18}F]FAZA is present in the intracellular compartment. The intracellular presence or absence of [^{18}F]FAZA is determined in this work to be due chiefly to the difference in k_4, i.e., the re-oxygenation of the reduced [^{18}F]FAZA, which is significantly elevated under sunitinib therapy. The perfused percentage of each tumor, as determined by the fbv, was found to be equal (within error margins) in each case, meaning that delivery of the radiotracer through the blood vessels is not impaired under sunitinib therapy. In summary, sunitinib treatment leads to decreased uptake in tumor cells due to increased re-oxygenation and back diffusion of [^{18}F]FAZA caused by overall lower hypoxia levels.

Congruent with the current findings, sunitinib also reduces [^{18}F]FMISO uptake by 22% to 35% in metastatic RCC patients [32]. The EGFR-blocker gefitinib showed even higher inhibition of [^{18}F]FAZA uptake (60% to 70%) in xenograft A431 human squamous cell carcinoma [37]. Similar observations with [^{18}F]FAZA and [^{18}F]FMISO were described in A431 tumor-bearing mice under therapy with CI-1033, a pan-Erb-B inhibitor [46]. Studies with [^{18}F]FDG analyzing glucose metabolism revealed 17% to 75% reduction in uptake during a sunitinib therapy [34-36], although with high variability for basic [^{18}F]FDG levels in RCC patients [47,48], reducing its utility in the clinics. In addition, the proliferation marker [^{18}F]FLT also showed a 16% reduced uptake in RCC patients in the presence of sunitinib [38]. Taken together, this supports the conclusion that systemic therapy with the TKI sunitinib achieves therapeutic efficacy by decreasing tumor hypoxia, metabolism, and proliferation. Monitoring of tumor oxygen levels is feasible in lesions with a well-defined population of hypoxic cells. This allows detection of reduced hypoxia during sunitinib therapy, while non-hypoxic metastases would not be expected to change [32].

Immunostaining with pimonidazole did only show a tendency for decreased binding to hypoxic cells in the short-term study. This may be explained by the short incubation time of only 1 h compared to 3 h in the long-term study. As the dynamic PET study reveals, effects of sunitinib on [^{18}F]FAZA are likewise not detectable at 1 h p.i. In theory, pimonidazole should behave similarly to [^{18}F]FAZA since both are 2-nitroimidazoles. Pimonidazole binding was reduced after 3 h p.i. by 30% which is similar to the 21% reduction of [^{18}F]FAZA. Considering the small numbers of animals, n, and thus relatively large SEM, this difference was insignificant. Immunohistochemistry with CD-31 and Ki67 resulted in a reduction in endothelial cells (and therefore mean vessel density and cell proliferation), pointing to a decrease in oxygen consumption and demand. This may have contributed to improved oxygenation of the sunitinib-treated Caki-1 tumors which correlates well with the fact that [^{18}F]FAZA delivery to the tumor cells was not impaired under sunitinib. From a clinical perspective, improved oxygenation has been shown to improve response to conventional chemotherapy, and radiotherapy, as well as reduce metastatic potential [49].

While sunitinib therapy leads to a pronounced reduction in tumor hypoxia, termination of therapy resulted in an increased hypoxia with even higher levels of [^{18}F]FAZA uptake compared to the control tumors. Following the release of TK inhibition, the tumor cell activity rebounds and experiences accelerated proliferation. This withdrawal flare phenomenon has not been thoroughly investigated subsequent to discontinuation of anti-angiogenic therapy. Similar rebound effects were observed in human renal cell cancer, where the SUV of [^{18}F]FLT increased by 15% after sunitinib withdrawal [38]. Currently, patients receive sunitinib in an on-and-off regimen [50]. Following treatment discontinuation, patients sometimes experience recurrent pain in metastatic sites, as a result of flare re-growth. It has been proposed that during this period of withdrawal, tumor cells are stuck in the 'S' phase and therefore are more vulnerable to combination cytotoxic chemotherapy [38]. This may be a useful strategy for therapy monitoring of RCC with PET, e.g., determining the hypoxia status.

Since direct effects of sunitinib on [^{18}F]FAZA uptake into the Caki-1 cells can be excluded from the *in vitro* studies, the observed reduction in tumor hypoxia *in vivo* must be related to other effects of sunitinib. Sunitinib was originally designed to specifically inhibit VEGFR, PDGFR, and C-kit; however, it has been found to inhibit other types of kinases as well, including non-receptor tyrosine kinases, receptor tyrosine kinases, tyrosine kinase-like kinases, cyclin-dependant kinases, and mitogen-activated protein kinase [11]. For this reason, it is reasonable to assume that sunitinib, as a type I TKI, has a greater number of off-target effects compared to some of the more specific TKIs categorized as type II, such as sorafenib and imatinib. This may help explain some contrasting effects observed in different cell lines following TKI therapy [33,47,51–53].

Conclusion

The present results show that [^{18}F]FAZA PET could be used to detect functional changes in the hypoxia status of renal cell carcinoma. It was found that during therapy with the TKI sunitinib, [^{18}F]FAZA uptake and trapping in Caki-1 tumors was reduced, indicating improved tumor oxygenation. Upon withdrawal of sunitinib therapy, [^{18}F]FAZA uptake into the tumor cells again increased, demonstrating a rebound in tumor hypoxia to even higher levels. This work demonstrates that [^{18}F]FAZA PET could be used to monitor TKI therapy clinically and may guide combination therapies dependent on tumor hypoxia status.

Competing interests
The authors declare that they have no competing interests.

Authors' contributions
DC, JM, LW, MW, and RM contributed to the concept and study design. DC, IM, and MW collected the data. DC and MW performed the data analysis. DC, JM, LW, MW, and RM were involved in the interpretation of the data. HSJ performed the kinetic analysis. All authors were involved in the writing process and all approved the manuscript before submission.

Acknowledgements
The authors would like to thank Dr. John Wilson, David Clendening, and Blake Lazurko from the Edmonton PET Center for providing ^{18}F produced on a biomedical cyclotron. In addition, we would like to thank Ali Akbari for the synthesis of [^{18}F]FAZA on an automated synthesis unit, Monica Wang for the help with the *in vitro* cell experiments, Kevin McCloy from the Technical Management Group at the Cross Cancer Institute (CCI) for maintenance of the small animal PET, and also Gail Hipperson and Dan McGinn from the Vivarium of the CCI for helping in the animal handling. This work was financially supported by the Edmonton PET Center, the Mr. Lube Foundation, and Alberta Innovates Health Solution (AIHS).

Author details
[1]Department of Oncology Cross Cancer Institute, University of Alberta, 11560 University Ave, Edmonton, Alberta Canada T6G 1Z2, Canada. [2]Department of Surgery, Walter C Mackenzie Health Sciences Centre, University of Alberta, 8440 112 Street, Edmonton, AB T6G 2B7, Canada.

Received: 13 February 2014 Accepted: 5 May 2014
Published online: 10 September 2014

References

1. Linehan WM, Walter MM, Zbar B: **The genetic base of cancer of the kidney.** *J Urol* 2003, **170:**163–172.
2. Tan PH, Cheng L, Rioux-Leclercq N, Merino MJ, Netto G, Reuter VE, Shen SS, Grignon DJ, Montironi R, Egevad L, Srigley JR, Delahunt B, Moch H: **Renal tumors: diagnostic and prognostic biomarkers.** *Am J Surg Pathol* 2013, **37:**1518–1531.
3. American Cancer Society: *Cancer Facts and Figures.* Atlanta ACS: American Cancer Society; 2013. http://www.cancer.org/Research/CancerFactsFigures/index. Accessed January 2014.
4. Cohen HT, McGovern FJ: **Renal-cell carcinoma.** *N Engl J Med* 2005, **353:**2477–2490.
5. Ljungberg B, Bensalah K, Bex A, Canfield S, Dabestani S, Hofmann F, Hora M, Kuczyk MA, Lam T, Marconi L, Merseburger AS, Mulders PFA, Staehler M, Volpe A: *Guidelines on Renal Cell Carcinoma.* Arnhem: European Association of Urology (EAU); 2013. http://www.uroweb.org/gls/pdf/10_Renal_Cell_Carcinoma_LR.pdf. Accessed January 2014.
6. Basu B, Eisen T: **Perspectives in drug development for metastatic renal cell cancer.** *Target Oncol* 2010, **5:**139–156.
7. Dutcher JP: **Recent developments in the treatment of renal cell carcinoma.** *Ther Adv Urol* 2013, **5:**338–353.
8. Schrader AJ, Hofmann R: **Metastatic renal cell carcinoma: recent advances and current therapeutic options.** *Anticancer Drugs* 2008, **19:**235–245.
9. Gross-Goupil M, Massard C, Ravaud A: **Targeted therapies in metastatic renal cell carcinoma: overview of the past year.** *Curr Urol Rep* 2012, **13:**16–23.
10. Zhang J, Yang PL, Gray NS: **Targeting cancer with small molecule kinase inhibitors.** *Nat Rev Cancer* 2009, **9:**28–39.
11. Mendel DB, Laird AD, Xin X, Louie SG, Christensen JG, Li G, Schreck RE, Abrams TJ, Ngai TJ, Lee LB, Murray LJ, Carver J, Chan E, Moss KG, Haznedar JO, Sukbuntherng J, Blake RA, Sun L, Tang C, Miller T, Shirazian S, McMahon G, Cherrington JM: **In vivo antitumor activity of SU11248, a novel tyrosine kinase inhibitor targeting vascular endothelial growth factor and platelet-derived growth factor receptors: determination of a pharmacokinetic/pharmacodynamic relationship.** *Clin Cancer Res* 2003, **9:**327–337.
12. Adams VR, Leggas M: **Sunitinib malate for the treatment of metastatic renal cell carcinoma and gastrointestinal stromal tumors.** *Clin Ther* 2007, **29:**1338–1353.
13. Petrelli A, Giordano S: **From single- to mutli-target drugs in cancer therapy: when aspecificity becomes an advantage.** *Curr Med Chem* 2008, **15:**422–432.
14. Wood L: **Sunitinib malate for the treatment of renal cell carcinoma.** *Expert Opin Pharmacother* 2012, **13:**1323–1336.
15. Escudier B, Albiges L, Sonpavde G: **Optimal management of metastatic renal cell carcinoma: current status.** *Drugs* 2013, **73:**427–438.
16. Castellano D, Ravaud A, Schmidinger M, De Velasco G, Vazquez F: **Therapy management with sunitinib in patients with metastatic renal cell carcinoma: key concepts and the impact of clinical biomarkers.** *Cancer Treat Rev* 2013, **39:**230–240.
17. Nilsson MB, Zage PE, Zeng L, Xu L, Cascone T, Wu HK, Saigal B, Zweidler-McKay PA, Heymach JV: **Multiple receptor tyrosine kinases regulate HIF-1alpha and HIF-2alpha in normoxia and hypoxia in neuroblastoma: implications for antiangiogenic mechanisms of multikinase inhibitors.** *Oncogene* 2010, **29:**2938–2949.
18. Marín-Hernández A, Gallardo-Pérez JC, Ralph SJ, Rodríguez-Enríquez S, Moreno-Sánchez R: **HIF-1alpha modulates energy metabolism in cancer cells by inducing over-expression of specific glycolytic isoforms.** *Mini Rev Med Chem* 2009, **9:**1084–1101.
19. Cassavaugh J, Lounsbury KM: **Hypoxia-mediated biological control.** *J Cell Biochem* 2011, **112:**735–744.
20. Chapman JD, Schneider RF, Urbain JL, Hanks GE: **Single-photon emission computed tomography and positron-emission tomography assays for tissue oxygenation.** *Semin Radiat Oncol* 2001, **11:**47–57.
21. Krohn KA, Link JM, Mason RP: **Molecular imaging of hypoxia.** *J Nucl Med* 2008, **49**(Suppl 2):129S–148S.
22. Sacco E, Pinto F, Totaro A, D'Addessi A, Racioppi M, Gulino G, Volpe A, Marangi F, D'Agostino D, Bassi P: **Imaging of renal cell carcinoma: state of the art and recent advances.** *Urol Int* 2011, **86:**125–139.
23. Krajewski KM, Giardino AA, Zukotynski K, Van den Abbeele AD, Pedrosa I: **Imaging in renal cell carcinoma.** *Hematol Oncol Clin North Am* 2011, **25:**687–715.
24. Carlin S, Humm JL: **PET of hypoxia: current and future perspectives.** *J Nucl Med* 2012, **53:**1171–1174.
25. Wuest M, Wuest F: **Positron emission tomography radiotracers for imaging hypoxia.** *J Labelled Comp Radiopharm* 2013, **56:**244–250.
26. Sorger D, Patt M, Kumar P, Wiebe LI, Barthel H, Seese A, Dannenberg C, Tannapfel A, Kluge R, Sabri O: **[^{18}F]Fluoroazomycinarabinofuranoside (18FAZA) and [^{18}F]Fluoromisonidazole (18FMISO): a comparative study of their selective uptake in hypoxic cells and PET imaging in experimental rat tumors.** *Nucl Med Biol* 2003, **30:**317–326.
27. Piert M, Machulla HJ, Picchio M, Reischl G, Ziegler S, Kumar P, Wester HJ, Beck R, McEwan AJ, Wiebe LI, Schwaiger M: **Hypoxia-specific tumor imaging with ^{18}F-fluoroazomycin arabinoside.** *J Nucl Med* 2005, **46:**106–113.
28. Reischl G, Dorow DS, Cullinane C, Katsifis A, Roselt P, Binns D, Hicks RJ: **Imaging of tumor hypoxia with [^{124}I]IAZA in comparison with [^{18}F]FMISO and [^{18}F]FAZA–first small animal PET results.** *J Pharm Pharm Sci* 2007, **10:**203–211.
29. Lewis JS, McCarthy DW, McCarthy TJ, Fujibayashi Y, Welch MJ: **Evaluation of 64Cu-ATSM in vitro and in vivo in a hypoxic tumor model.** *J Nucl Med* 1999, **40:**177–183.
30. Dunphy MP, Lewis JS: **Radiopharmaceuticals in preclinical and clinical development for monitoring of therapy with PET.** *J Nucl Med* 2009, **Suppl 1:**106S–121S.
31. Valable S, Petit E, Roussel S, Marteau L, Toutain J, Divoux D, Sobrio F, Delamare J, Barré L, Bernaudin M: **Complementary information from magnetic resonance imaging and (18)F-fluoromisonidazole positron emission tomography in the assessment of the response to an antiangiogenic treatment in a rat brain tumor model.** *Nucl Med Biol* 2011, **38:**781–793.
32. Hugonnet F, Fournier L, Medioni J, Smadja C, Hindié E, Huchet V, Itti E, Cuenod CA, Chatellier G, Oudard S, Faraggi M: **Metastatic renal cell carcinoma: relationship between initial metastasis hypoxia, change after 1 month's sunitinib, and therapeutic response: an ^{18}F-fluoromisonidazole PET/CT study.** *J Nucl Med* 2011, **52:**1048–1055.
33. Murakami M, Zhao S, Zhao Y, Chowdhury NF, Yu W, Nishijima K, Takiguchi M, Tamaki N, Kuge Y: **Evaluation of changes in the tumor microenvironment after sorafenib therapy by sequential histology and ^{18}F-fluoromisonidazole hypoxia imaging in renal cell carcinoma.** *Int J Oncol* 2012, **41:**1593–1600.

34. Revheim ME, Winge-Main AK, Hagen G, Fjeld JG, Fosså SD, Lilleby W: **Combined positron emission tomography/computed tomography in sunitinib therapy assessment of patients with metastatic renal cell carcinoma.** *Clin Oncol (R Coll Radiol)* 2011, **23:**339–343.
35. Vercellino L, Bousquet G, Baillet G, Barré E, Mathieu O, Just PA, Desgrandchamps F, Misset JL, Hindié E, Moretti JL: **^{18}F-FDG PET/CT imaging for an early assessment of response to sunitinib in metastatic renal carcinoma: preliminary study.** *Cancer Biother Radiopharm* 2009, **24:**137–144.
36. Lyrdal D, Boijsen M, Suurküla M, Lundstam S, Stierner U: **Evaluation of sorafenib treatment in metastatic renal cell carcinoma with 2-fluoro-2-deoxyglucose positron emission tomography and computed tomography.** *Nucl Med Commun* 2009, **30:**519–524.
37. Solomon B, Binns D, Roselt P, Weibe LI, McArthur GA, Cullinane C, Hicks RJ: **Modulation of intratumoral hypoxia by the epidermal growth factor receptor inhibitor gefitinib detected using small animal PET imaging.** *Mol Cancer Ther* 2005, **4:**1417–1422.
38. Liu G, Jeraj R, Vanderhoek M, Perlman S, Kolesar J, Harrison M, Simoncic U, Eickhoff J, Carmichael L, Chao B, Marnocha R, Ivy P, Wilding G: **Pharmacodynamic study using FLT PET/CT in patients with renal cell cancer and other solid malignancies treated with sunitinib malate.** *Clin Cancer Res* 2011, **15**(17):7634–7644.
39. Bruce JY, Kolesar JM, Hammers H, Stein MN, Carmichael L, Eickhoff J, Johnston SA, Binger KA, Heideman JL, Perlman SB, Jeraj R, Liu G: *A phase I pharmacodynamic trial of sequential sunitinib with bevacizumab in patients with renal cell carcinoma and other advanced solid malignancies. Cancer Chemother Pharmacol* 2014. doi:10.1007/s00280-013-2373-9.
40. Reischl G, Ehrlichmann W, Bieg C, Solbach C, Kumar P, Wiebe LI, Machulla H-J: **Preparation of the hypoxia imaging PET tracer [^{18}F]FAZA: reaction parameters and automation.** *Appl Radiat Isot* 2005, **62:**897–901.
41. Verwer EE, van Velden FHP, Bahce I, Yaqub M, Schuit RC, Windhorst AD, Raijmakers P, Lammertsma AA, Smit EF, Boellaard R: **Pharmacokinetic analysis of [18F]FAZA in non-small cell lung cancer patients.** *Eur J Nucl Med Mol Imaging* 2013, **40:**1523–1531.
42. Koch CJ, Stobbe CC, Baer KA: **Metabolism induced binding of ^{14}C-misonidazole to hypoxic cells: kinetic dependence on oxygen concentration and misonidazole concentration.** *Int J Radiat Oncol Biol Phys* 1984, **10:**1327–1331.
43. Houk BE, Bello CL, Poland B, Rosen LS, Demetri GD, Motzer RJ: **Relationship between exposure to sunitinib and efficacy and tolerability endpoints in patients with cancer: results of a pharmacokinetic/pharmacodynamic metaanalysis.** *Cancer Chemother Pharmacol* 2010, **66:**357–371.
44. Maier FC, Kneilling M, Reischl G, Cay F, Bukala D, Schmid A, Judenhofer MS, Röcken M, Machulla HJ, Pichler BJ: **Significant impact of different oxygen breathing conditions on noninvasive in vivo tumor-hypoxia imaging using [^{18}F]-fluoro-azomycinarabino-furanoside ([^{18}F]FAZA).** *Radiat Oncol* 2011, **6:**165–175.
45. Rischin D, Hicks RJ, Fisher R, Binns D, Corry J, Porceddu S, Peters LJ: **Prognostic significance of [^{18}F]-misonidazole positron emission tomography-detected tumor hypoxia in patients with advanced head and neck cancer randomly assigned to chemoradiation with or without tirapazamine: a substudy of Trans-Tasman Radiation Oncology Group Study 98.02.** *J Clin Oncol* 2006, **24:**2098–2104.
46. Dorow DS, Cullinane C, Conus N, Roselt P, Binns D, McCarthy TJ, McArthur GA, Hicks RJ: **Multi-tracer small animal PET imaging of the tumour response to the novel pan-Erb-B inhibitor CI-1033.** *Eur J Nucl Med Mol Imaging* 2006, **33:**441–452.
47. Majhail NS, Urbain JL, Albani JM, Kanvinde MH, Rice TW, Novick AC, Mekhail TM, Olencki TE, Elson P, Bukowski RM: **F-18 fluorodeoxyglucose positron emission tomography in the evaluation of distant metastases from renal cell carcinoma.** *J Clin Oncol* 2003, **21:**3995–4000.
48. Dilhuydy MS, Durieux A, Pariente A, de Clermont H, Pasticier G, Monteil J, Ravaud A: **PET scans for decision-making in metastatic renal cell carcinoma: a single-institution evaluation.** *Oncology* 2006, **70:**339–344.
49. Arabi M, Piert M: **Hypoxia PET/CT imaging: implications for radiation oncology.** *Q J Nucl Med Mol Imaging* 2010, **54:**500–509.
50. Atkinson BJ, Kalra S, Wang X, Bathala T, Corn P, Jonasch E: *Clinical outcomes in patients with metastatic renal cell carcinoma treated with alternative sunitinib schedules. J Urol: Tannir NM* 2013. doi:10.1016/j.juro.2013.08.090.
51. Murakami M, Zhao S, Zhao Y, Yu W, Fatema CN, Nishijima KI, Yamasaki M, Takiguchi M, Tamaki N, Kuge Y: **Increased intratumoral fluorothymidine uptake levels following multikinase inhibitor sorafenib treatment in a human renal cell carcinoma xenograft model.** *Oncol Lett* 2013, **6:**667–672.
52. Gaustad JV, Simonsen TG, Leinaas MN, Rofstad EK: **Sunitinib treatment does not improve blood supply but induces hypoxia in human melanoma xenografts.** *BMC Cancer* 2012, **12:**388–403.
53. Gaustad JV, Simonsen TG, Roa AM, Rofstad EK: **Tumors exposed to acute cyclic hypoxia show increased vessel density and delayed blood supply.** *Microvasc Res* 2013, **85:**10–15.

doi:10.1186/s13550-014-0027-5
Cite this article as: Chapman *et al.*: Detecting functional changes with [^{18}F]FAZA in a renal cell carcinoma mouse model following sunitinib therapy. *EJNMMI Research* 2014 **4**:27.